Bioorganic & Medicinal Chemistry 22 (2014) 5569–5577

Contents lists available at ScienceDirect

Bioorganic & Medicinal Chemistry

journal homepage: www.elsevier.com/locate/bmc

Characterization of the *N*-oxygenase AurF from *Streptomyces thioletus*

Emmanuel Chanco [a], Yoo Seong Choi [b], Ning Sun [c], Michael Vu [b], Huimin Zhao [b,*]

[a] Department of Chemistry, University of Illinois at Urbana–Champaign, 600 S. Mathews Avenue, Urbana, IL 61801, USA
[b] Department of Chemical and Biomolecular Engineering, University of Illinois at Urbana–Champaign, 600 S. Mathews Avenue, Urbana, IL 61801, USA
[c] Department of Biochemistry, University of Illinois at Urbana–Champaign, 600 S. Mathews Avenue, Urbana, IL 61801, USA

ARTICLE INFO

Article history:
Received 17 April 2014
Revised 29 May 2014
Accepted 1 June 2014
Available online 12 June 2014

Keywords:
AurF
N-Oxygenation
Diiron monooxygenase
Biocatalysis
Electron transfer

ABSTRACT

AurF catalyzes the *N*-oxidation of *p*-aminobenzoic acid to *p*-nitrobenzoic acid in the biosynthesis of the antibiotic aureothin. Here we report the characterization of AurF under optimized conditions to explore its potential use in biocatalysis. The pH optimum of the enzyme was established to be 5.5 using phenazine methosulfate (PMS)/NADH as the enzyme mediator system, showing ~10-fold higher activity than previous reports in literature. Kinetic characterization at optimized conditions give a K_m of 14.7 ± 1.1 μM, a k_{cat} of 47.5 ± 5.4 min^{-1} and a k_{cat}/K_m of 3.2 ± 0.4 μM^{-1} min^{-1}. PMS/NADH and the native electron transfer proteins showed significant formation of the *p*-hydroxylaminobenzoic acid intermediate, however H_2O_2 produced mostly *p*-nitrobenzoic acid. Alanine scanning identified the role of important active site residues. The substrate specificity of AurF was examined and rationalized based on the protein crystal structure. Kinetic studies indicate that the K_m is the main determinant of AurF activity toward alternative substrates.

1. Introduction

The nitro group is a common functional group present in many industrially important commodity chemicals, pharmaceuticals, and explosives. Nitro-containing compounds in the environment are typically encountered as pollutants and xenobiotic compounds, and have been implicated in several types of DNA damage and cancer; thus, biodegradation of these compounds is an important area of research. However, the biosynthesis of naturally occurring nitro compounds is not well understood. Several important nitro-containing natural products such as stephanosporin, pyrrolonitrin, and chloramphenicol, are produced by various organisms as antibiotics, signaling molecules or other types of metabolites (Fig. 1A).[1–3] The mechanism for installation of nitro groups in several compounds is known, such as the production of nitrotyrosine through free radical reactions of peroxonitrate, and the *N*-oxygenation of pyrrolonitrin by the enzyme PrnD via hydroxylamine and nitroso intermediates.[1,2,4] Much of the interest in biosynthetic nitration is due to the gentle conditions and benign waste produced in comparison to the harsh conditions necessary for chemical nitration. Additionally, enzyme-based nitration provides a way to precisely control regiospecificity, a task that can be sometimes difficult in chemical synthesis. Therefore, characterization of enzymes which catalyze nitro group formation is of interest for green chemistry, biochemical synthesis and in the development of pharmaceuticals and niche chemicals.

AurF is a diiron monooxygenase from *Streptomyces thioletus* that catalyzes the production of *p*-nitrobenzoic acid (PNBA) from *p*-aminobenzoic acid (PABA) via *p*-hydroxylaminobenzoic acid (PHABA). This precursor is used as a starter unit by *S. thioletus* for the synthesis of the polyketide antibiotic aureothin. Like PrnD, *N*-oxygenation is the mechanism used by AurF (Fig. 1B). Several properties of the enzyme such as its regiospecificity, mild reaction conditions, heterologous expression and activity in *Escherichia coli*, have made this enzyme attractive for biotechnology applications and as a complement to chemical syntheses. Much work has been carried out by the Zhao, Bollinger, and Hertweck groups in characterizing this enzyme such as determination of the active metal and crystal structure, elucidation of its mechanism, and progress in understanding its substrate specificity.[2,5–12] However, several pieces of data are contradictory, including substrate specificity of the enzyme as well as mechanistic considerations. Additionally, much of the literature data comes from the use of a manganese-enriched form of AurF which has a different active site structure compared to the diiron enzyme.[5,12,13] Finally, the low activity of AurF has also hampered its characterization. Thus, in this report, we performed detailed characterization of AurF under optimized

* Corresponding author. Tel.: +1 217 333 2631; fax: +1 217 333 5052.
E-mail address: zhao5@illinois.edu (H. Zhao).

http://dx.doi.org/10.1016/j.bmc.2014.06.002
0968-0896/

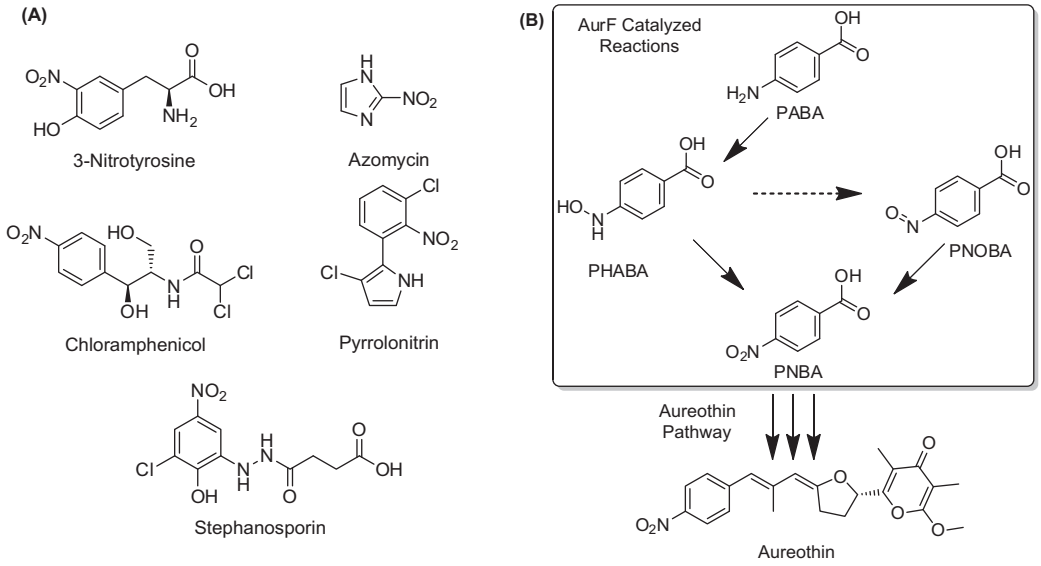

Figure 1. (A) Nitro-containing compounds derived from natural sources. (B) *N*-Oxygenation catalyzed by AurF proceeds via hydroxylamine and possibly nitroso intermediates, with nitro product serving as the starter unit for biosynthesis of the polyketide aureothin.

assay conditions, including enzyme kinetics, mutagenesis of active site residues, and an analysis of the enzyme's substrate specificity. The resulting insights should facilitate its optimization and engineering as a new biocatalyst for practical applications.

2. Materials and methods

2.1. Cloning and library creation

Restriction enzymes and DNA polymerases used were from New England Biolabs. Plasmids containing AurF used in this study were identical to previous constructs from literature.[5,10] AurF point mutants and saturation mutagenesis libraries were created by overlap extension-PCR (OE-PCR) using primers containing the mutation of interest. These inserts were digested by HindIII and NcoI, ligated into a similarly digested pTrc99a plasmid, and electroporated into *E. coli*. Mutations were confirmed by DNA sequencing.

2.2. Enzyme purification

E. coli BL21 (DE3) cells containing a pTrc99a-6His-AurF plasmid were grown at 37 °C in Terrific Broth media and 100 μg/mL ampicillin. Cultures were induced at an OD_{600} of 0.6 with IPTG (final concentration 100 μM) and grown overnight at 25 °C. Cells were centrifuged and resuspended in a pH 7.4 buffer containing 20 mM NaH_2PO_4, 300 mM NaCl and 20 mM imidazole. The cells were then lysed by sonication and protein was purified via nickel affinity chromatography. Concentration and buffer exchange was performed by diafiltration with a 10 kDa Amicon filter, and aliquots of the enzyme was stored at −80 °C in a buffer containing 20 mM NaH_2PO_4, 300 mM NaCl and 20% glycerol at pH 8.0. Enzyme concentration was determined by the BioRad Quickstart Bradford assay (BioRad, Hercules, CA) using bovine serum albumin as a standard. As a comparison, a Pierce BCA Protein assay kit (Thermo Fisher Scientific, Rockford, IL) was used with identical standards as the Bradford assay. AurF quantified by the Bradford assay gives approximately twice the enzyme concentration compared to the previously used commercial BCA kit (Fig. S1) using identical standards. In this work, we report all our specific activity, k_{cat} and k_{cat}/K_m multiplied by a correction factor of 2.05 (Fig. S1) to be consistent with the BCA assay used in previous AurF literature; however we report enzyme concentrations based on the Bradford assay. Purification of ferredoxin and ferredoxin-NADP reductase was as previously reported.[5]

2.3. Enzymatic assay

All reagents and compounds tested were obtained either from Sigma–Aldrich, TCI America, Matrix Scientific or Acros Organics. The pH assay was performed at 20 °C with a final volume of 1 mL in the McIlvane buffer, using stock solutions of 40 mM NaH_2PO_4 and 20 mM citric acid (5× dilution of the originally listed stock solutions).[14] The final assay mixture contained 0.5–2 μM AurF, 75 μM phenazine methosulfate (PMS), 750 μM NADH and 100 μM of PABA in the McIlvane buffer. Addition of NADH initiated the reaction, with timepoints taken every 30 s. Reactions were quenched by addition of 20 μL of 5% (v/v) trifluoroacetic acid which gives a final pH of approximately 2. Depletion of substrate was used to quantify the reaction rate. Specific activity of the enzyme was fitted to the following equation to find the pK_a of the groups responsible for the pH dependence of the enzyme.[15]

$$v = \frac{V_{max}}{\frac{10^{-pH}}{10^{-pK_{a1}}} + \frac{10^{-pK_{a2}}}{10^{-pH}} + 1}$$

For the rest of the assays, 20 mM MES buffer at pH 5.5 was used instead of the McIlvane buffer for the sake of convenience. NADH and PMS concentrations used were identical to the previous reactions. For kinetic determination of the wild type enzyme, 2.5–100 μM of PABA with 0.2 μM of enzyme was used, taking timepoints every 30 s. Kinetic parameters were obtained by fitting the Michaelis–Menten equation to the data using Origin 8 (OriginLab, Northampton, MA). For the alternate substrates assay, 2–20 μM of AurF and 250 μM of substrate were used, with timepoints taken every 60 s for 3 min. Mutant and alternate substrate kinetic characterization followed their respective timepoints, with substrate concentrations ranging from 15 to 400 μM. Negative controls containing no enzyme were also tested, with rates from non-enzymatic depletion of substrate subtracted from the assayed data. The peroxide-based assays were similar to the ones using the

alternate substrates, using a final concentration of 20 μM enzyme and 1.2% H_2O_2, and omitting the NADH and PMS. Assays based on ferredoxin/ferredoxin-NADPH reductase used 5 μM AurF, 25 μM ferredoxin, 5 μM ferredoxin-NADPH reductase and 750 μM NADPH.

2.4. In vivo AurF analysis

Cells were grown and induced in a manner similar to the cells used in enzymatic purification of AurF. Cells were then centrifuged and resuspended in assay buffer to a final OD_{600} of 10.[10] Substrate was added to a final concentration of 500 μM to 25 mL of the resuspended cells, and timepoints were taken after several hours. Cells containing an empty pTrc99a vector were grown and tested in identical conditions and served as a negative control.

2.5. HPLC analysis

Analysis was performed on an Agilent 1100 HPLC using a 3.5 μm Zorbax SB-C18 column (3.0 mm × 150 mm). For kinetic characterization and mutant analysis, the following method was used: solvent A: 1% acetic acid, solvent B: methanol. Flow rate 0.5 mL/min. The gradient was as follows: 0–7 minutes: 90%A, 8.5 min: 75%A, 10 min: 25% A, 14–23 min: 90%A. PABA and PNBA were quantified at 290 nm and 268 nm, respectively. For LC–MS analysis, an Agilent 1100 LC/MSD Trap XCT Plus was used with identical conditions as above, but with a flow rate of 350 μL/min. APCI was used as an ionization source, with the following parameters: Nebulizer pressure: 60 psi; Drying gas flow: 7 L/min; Drying gas temp: 350 °C; APCI vap temp: 400 °C; Capillary voltage: 3500 V. For alternate substrates, a similar method was used; however an ion-pairing reagent (2 mM sodium 1-heptane sulfonate) was added to each buffer, and a lower flow rate (0.4 mL/min) was used for good separation of the compounds. Compounds were detected using wavelengths of 240, 250, 268, 290, 320, and 380 nm and quantified via comparison to a standard curve.

2.6. Docking/modelling studies

Visualization and modelling studies were performed using VMD.[16] For docking studies, PDB files with structure IDs 3CHH (AurF) and 1QT9 (ferredoxin) were submitted to the ClusPro server (http://cluspro.bu.edu/), docked and scored.[17]

2.7. Synthesis of PHABA

PHABA was synthesized according to previously described literature,[9] except that 1.6 equiv of Zn were used instead of 2 to prevent overreduction to PABA. PHABA was then purified via flash chromatography on silica with ethyl acetate as a solvent. The compound was verified by LC/MS and comparison to PHABA produced by AurF.

3. Results and discussion

3.1. pH dependence

Early reports from 1965 regarding AurF suggested that the pH optimum of the enzyme occurred under neutral conditions. However, this involved an in vivo assay using whole cells of *S. thioletus*, the results of which more likely reflect the pH dependence of the organism rather than actual enzymatic activity.[18] Under our assay conditions using PMS/NADH as a reduction system, the optimum pH of AurF was determined to be pH 5.5 with significant activity seen between pH 4.5 and 6.5 (Fig. 2A). However, when AurF was tested at pH 7.5 and 5.5 with either ferredoxin/ferredoxin-NADP$^+$

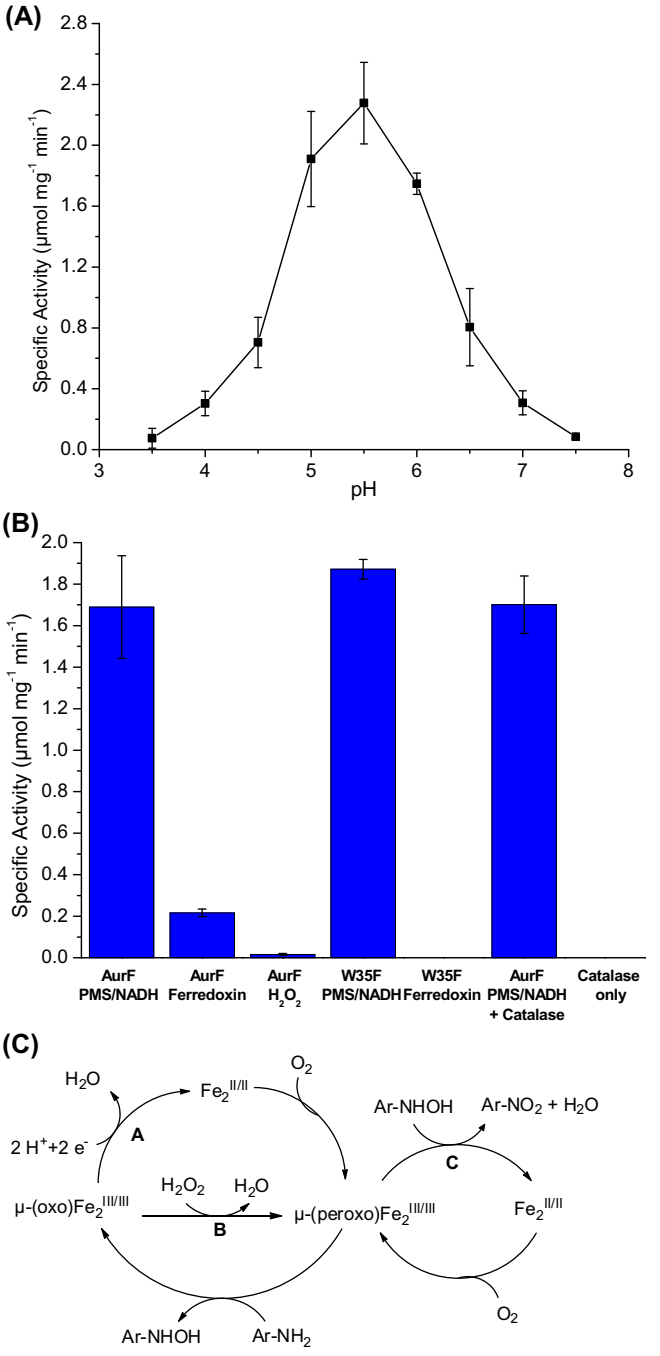

Figure 2. (A) pH dependence of AurF with 100 μM of PABA. (B) Specific activity of AurF and W35F mutant using various reductants using 250 μM of PABA. The effect of catalase on PMS/NADH was also examined. (C) Proposed reaction cycle for AurF.

reductase (Fd/FDR) or H_2O_2 as reductants, the activity of AurF was fairly constant, and did not change as significantly as in the case of PMS/NADH (Fig. S2). pH 5.5 as an optimum is unusual, given that a recent paper by Sazinsky and co-workers on an *N*-oxygenase (23% sequence identity to AurF) from *Pseudomonas syringae* showed a pH optimum of 9.0–9.5, albeit using peroxide as a reductant.[19] While the increased activity using PMS/NADH at lower pH could simply be due to more favorable protonation/redox state of PMS, the higher activity can also be interpreted in terms of the catalytic mechanism of AurF. Fitting the pH profile of AurF to an equation (see Materials and Methods section) gives the pK_a of catalytically or structurally important residues, and it was found

that these residues had pK_as of 4.6 and 6.4, which likely correspond to an aspartate/glutamate and a histidine residue, respectively.

While the pH optimum of AurF at pH 5.5 using PMS/NADH is unmistakable, it is unlikely that this is the pH at which the reaction occurs in vivo. Although *Streptomyces* species have been shown to be able to grow and sporulate under low pH conditions depending on media conditions and strains, the internal pH of the cell should be close to neutral or somewhat basic (pH 6.5–8.5).[20,21] Additionally, required accessory proteins such as ferredoxin may show decreased or no activity at this lower pH (although this was compensated for in vitro assays with the large amounts of ferredoxin and reductase used). Finally, a related enzyme CmlI, which also catalyzes a similar *N*-oxidation in the chloramphenicol biosynthesis pathway, does not show increased activity at this pH (unpublished data), and several other structurally-related diiron enzymes have been found to have optimal pH values at physiological values.[22–24] At this point, it is likely that some combination of both enzymatic features of AurF and the redox properties of PMS that provide this pH optimum.

3.2. Kinetic characterization

AurF was characterized at pH 5.5 to have a K_m of 14.7 ± 1.1 μM, a k_{cat} of 97.4 ± 11.1 min^{-1} and a k_{cat}/K_m of 6.6 ± 0.8 μM^{-1} min^{-1} (Fig. S3). This is interesting in comparison to data reported in literature at pH 7.5, with a K_m of 8.89 ± 0.87 μM, k_{cat} of 5.04 ± 0.22 min^{-1}, and k_{cat}/K_m of 0.57 ± 0.03 min^{-1} μM^{-1}.[5] The values for K_m are similar at both pHs suggesting no major changes in the active site/binding mechanism over different pHs, however the 19-fold increase in k_{cat} at pH 5.5 compared to that at pH 7.5 suggests that a proton transfer is rate-limiting.

Several possibilities can account for this increase in k_{cat} at a lower pH. The proposed mechanism of AurF as developed by Bollinger and co-workers requires the formation of a hydroperoxide bound to the diiron center of the protein.[7,9] The initial peroxo complex can be formed by reaction of oxygen and Fe_2(II/II), and subsequently be protonated to the hydroperoxo intermediate. In this mechanism, attack of the aromatic amine on the hydroperoxo electrophile could enable the formation of the initial hydroxylamine intermediate of PABA. Although this process could also proceed with nucleophilic attack on the peroxo complex and subsequent protonation, the hydroperoxo species is a stronger electrophile, and would more readily be attacked by the amine nucleophile. Another case is the possible protonation of active-site carboxylates and histidines affecting either the reaction or electron transfer pathway. Several aspartate, glutamate and histidine residues are found in the active site of AurF, and may perform some catalytic roles relying on proton transfer. The pK_a's of these residues are approximately 4 and 6 for aspartate/glutamate and histidine, respectively, and their proximity to both the diiron cluster and the active site cavity suggests their importance in the activity of the enzyme. Alanine mutations of these residues have been shown to deactivate the enzyme, underlying their importance.[9,25] Calculations performed by Jayapal and Rajaraman have shown the protonation of E196 and E277 significantly affects the geometry and reactivity of the AurF's active site.[13] In particular, residue E196 binds to one of the iron atoms as a unidentate ligand, and results from literature suggest that it may function as a general base to abstract protons generated by the reaction.

Although the *N*-oxygenation activity of AurF has been demonstrated in several laboratories, the specific activity measured in our case is typically much higher compared to results from other laboratories. Notably, the in vitro specific activity found in our conditions for the wild type enzyme was 1.99 ± 0.27 and 0.148 ± 0.053 μmol mg^{-1} min^{-1} at pH 5.5 and 7.5, respectively, with 100 μM of PABA, while the highest activity seen in literature is 0.0032 μmol mg^{-1} min^{-1} at pH 7.5.[5,12] We also assayed AurF using a peroxide-shunt method at pH 5.5 and found a specific activity of 0.0162 ± 0.0043 μmol mg^{-1} min^{-1}, indicating that while the lower pH increases the activity of the enzyme (5–13×), the method for delivering reductive equivalents to the enzyme provides significantly higher enhancements to activity (50–122×). We previously attributed the differences in enzymatic activity between our results and results by Zocher et al. to the metal in the active site, but it may also be the case that the source of the reducing equivalents is more important.[12] In the experiments performed by the Sazinsky and Hertweck groups, the source of electrons used for the assay is hydrogen peroxide at physiological or basic pH, using a peroxide shunt-type mechanism to enable catalysis by the active site. However, it has been demonstrated for the diiron enzyme toluene 4-monooxygenase hydroxylase that the use of the peroxide shunt is ~600-fold slower than the use of the native electron mediator proteins.[26] The reaction of PMS and NADH has been reported to produce superoxide and hydrogen peroxide, so to observe any contributions by a peroxide shunt mechanism, 50 units of catalase were added to a typical reaction system.[27,28] No difference in activity was observed compared to reactions without catalase, indicating that the PMS/NADH system proceeds via a different mechanism than the peroxide-based method (Fig. 2C). It has also been noted that the PMS/NADH system can perform hydroxylations of aromatic systems; however no such activity was observed in our reactions.[28]

3.3. Electron transfer pathway

It was shown that the AurF electron transfer pathway resembles the one from the ribonucleotide-reductase pathway, using native ferredoxin-type enzymes as electron mediators.[29] We previously used PMS and NADH to reconstitute the activity of AurF, and we wanted to see whether PMS/NADH also uses the same electron-transfer pathway as the ferredoxin-based method. Incidentally, the PMS/NADH system has also been reported to allow a structurally similar non-heme diiron enzyme to turnover substrates faster than even ferredoxin-based methods.[30] To that end, we tested a few different mutants (R38A/G, W35A/F) based on the docking studies of AurF with ferredoxin. Out of the mutants tested, only W35F was soluble, and was assayed using both ferredoxin/ferredoxin-NADP reductase and PMS/NADH. The W35F mutant has previously been reported to be inactive in vivo due to disruption of the ferredoxin-AurF electron-transfer pathway, but active in vitro via a peroxide-shunt mechanism.[29] No activity was seen using the ferredoxin-based system, but with the PMS/NADH system, activity comparable to the native enzyme was seen (Fig. 2B). This suggests that the PMS/NADH system reconstitutes the enzyme not through the complete ferredoxin pathway, either bypassing W35, or through some different mechanism.

Although the PMS/NADH system may not proceed through the native electron transfer pathways, the product distribution of AurF using this system is similar to the native electron transfer pathways in vitro, while the peroxide shunt mechanism provides a different product distribution. Accumulation of the hydroxylamine intermediate is observed in vivo and the in vitro ferredoxin/NADPH-reductase and PMS/NADH systems, while the primary product of the peroxide shunt is the final nitro product (Table 1 and Fig. S4). It has previously been observed that in vitro, the peroxide-shunt mechanism produces slightly more of the nitro product than the hydroxylamine intermediate, while an in vivo experiment showed that the PHABA accumulates in greater than 12-fold excess compared to the nitro product.[12] It may be the case that in the peroxide shunt mechanism, the initial conversion of PABA to PHABA is a slow step; while in the other systems tested, the conversion of PHABA to PNBA is rate limiting. This would

Table 1
Product distribution of AurF using various reduction mechanisms

	PABA (μM)	PHABA (μM)	PNBA (μM)
Ferredoxin (5 μM AurF)	191.0 ± 4.7	36.9 ± 0.5	6.8 ± 1.6
PMS/NADH (0.5 μM AurF)	214.0 ± 2.4	27.0 ± 3.4	8.3 ± 1.4
H_2O_2 (20 μM AurF)	245.6 ± 2.6	0.2 ± 0.02	5.3 ± 0.3

Reaction conditions were 105 s reactions using 250 μM of PABA at pH 5.5. Reactions were performed in triplicate, except for ferredoxin PHABA, which was only quantified in duplicate due to coelution issues.

explain the differences in product distribution for the peroxide shunt and the other systems. Analogous to the mechanisms found in other diiron enzymes, the peroxide shunt mechanism relies on the formation of a μ-(peroxo)diferric intermediate from a μ-(oxo)diferric state, bypassing the diferrous state (Fig. 2C).[25,26,31] If the rate of μ-(peroxo)$Fe_2^{III/III}$ generation is much slower through the peroxide shunt mechanism (Step B in Fig. 2C) than the Ar-NHOH → Ar-NO_2 conversion (Step C), then whatever hydroxylamine generated is converted to the nitro compound rapidly. Li et al. have shown that conversion of PHABA to PNBA only requires the addition of oxygen to AurF, and does not require the input of electrons to effect the reaction. However, if step A (the reaction pathway used by ferredoxin and presumably PMS/NADH) is faster or goes at the same rate as step C, the accumulation of the hydroxylamine will occur. It is unclear why the peroxide shunt is slower in AurF, but similar results from T4MOH suggest H_2O_2 must lose its hydrogens before binding to the diiron center can occur, or that binding of the peroxide distorts the active site and slows the oxygenation reaction.[26]

3.4. Mutational analysis

To determine which residues are important for catalysis or substrate recognition in AurF, alanine scanning was performed on several different residues in the active site (Fig. 3A–E). In most cases, important trends could be observed, while in a few others, the activity relationship could not be easily defined. The crystal structure of diiron AurF gives several hints as to the structural role of important active site residues (Fig. 3A and B). The minor difference in K_m over a 2 pH unit range suggests that the substrate recognition is dependent mostly on residues that do not change their ionization within the pH range of the enzyme. The only protonatable groups that do not complex the active metals are residues D135, D226, H143 and H223, and these four do not directly interact with the native substrate.

Alanine mutation of residues directly surrounding the substrate (Y93, V97, T100, N200, or R302) decreases the activity of AurF to 50% or less of the wildtype. Y93, N200 and R302 are responsible for recognition and binding the carboxylate end of the native substrate either directly or through water-mediated contacts; however, none of these residues are completely essential for AurF activity, indicating some redundancy in the carboxylate recognition (Fig. 3A and B). Comparison with several homologs shows that in general, residues with sidechains that can participate in hydrogen bonding are favored at these positions (Table S1). Residues directly adjacent to the aromatic ring (V97 and T100) also show similar reductions in activity. These residues delineate the side and the top of the active site, respectively, and mutation of these residues to alanine could allow the substrate to drift farther away from the diiron center or alter the structure of the active site. However, it could also be argued that an alanine mutation at these sites would not be a sufficiently drastic mutation from the previous mutation; V97 is situated facing the aromatic ring, and one methyl group could conceivably be enough to align the substrate to the metal center. The T100 residue's counterpart in a few AurF homologs is actually alanine (Table S1), which indicates that at best T100A is a conservative mutation. The relatively smaller decrease in AurF activity for this alanine mutant collaborates this fact. Thus, the decrease in activity for these mutants is surprising considering the relatively minor steric change from the wild type residues.

Modelling the rotamers of the N94 residue indicates that it may be involved in modulation of the redox activity of the active metals (Fig. 3C) by orienting residues H143 and H223. Similar Asp-His couples mediate enzyme activity in peroxidases by modulating the pK_a of the histidine residue.[32,33] A BLAST search revealed that N94 is very strongly conserved through several probable AurF-type enzymes (Table S1), with the histidines also being well-conserved. Substitution with alanine shows a sharp decrease of activity, however activity was not completely abolished, indicating that this residue may function in a structural role rather than as a modulator of electron transfer or redox. This is corroborated by the observation that mutation of this residue to alanine caused an sharp decrease in solubility of the protein, suggestive of misfolding or instability. Similar results on AurF insolubility have been observed for residues related to the electron transfer of AurF (W35A and D135A).[29]

The activities of mutations R96A, I199A, L203A and F264 are more difficult to explain. The R96A mutant was previously reported in literature not to have activity in vivo, but according to our results, show around 75% activity.[12] Zocher et al. rationalized that this arginine was important in the carboxylate binding of AurF of AurF and by removal of this functionality the enzyme would be deactivated. This was supported by their crystal structure of the dimanganese version of AurF. However, in the diiron version of AurF, R96 is oriented away from the active site and does not directly bind the substrate. That is not to say that the residue plays no role in binding; it may assist in water-mediated contacts to the substrate, or be flexible enough to bind directly as evidenced by the small drop (around 25%) in activity compared to the wild type. Residue I199 lines the cavity of the active site and separates it from the exterior of the protein. Although somewhat far from the substrate (6.8 Å), this residue walls off two water molecules that constrain the substrate. Mutation to alanine undermines the structure of the active site by creating an opening accessible to bulk solvent. Strongly conserved residue L203 forms the 'floor' of the AurF active site, and mutating it to an alanine halves the activity of the enzyme. Similar to V97, the most likely role of this residue is to restrict the substrate in the active site. While Y93 and N200 provide significant hydrogen bonding to PABA to restrain it in the binding pocket, L203 complements this binding by providing a physical barrier below the substrate. Similar to R96, the positioning of F264 is quite different in the diiron and dimanganese versions of AurF. In the dimanganese enzyme, F264 aligns parallel to PABA and acts to align it to the active site, while in the diiron version, F264 is ~7 Å away from the substrate and is perpendicular to the PABA aromatic ring. As this residue is located next to R302, the F264A mutation allows the R302 residue to shift position, disrupting its water-mediated contacts with the substrate. This leads to the 50% decrease in activity for this mutant.

3.5. Substrate specificity of AurF

The substrate specificity of AurF was tested with a variety of different compounds (Fig. 4A and B) at high substrate concentrations in order to saturate the enzyme. In general, our results show similar trends to literature but with higher activity due to optimized assay conditions.[11] In certain cases, significant exceptions were observed. The native substrate PABA (**1**) has a specific activity of 1.68 ± 0.25 μmol mg^{-1} min^{-1} at a concentration of 250 μM of substrate, indicating some slight substrate inhibition compared to the

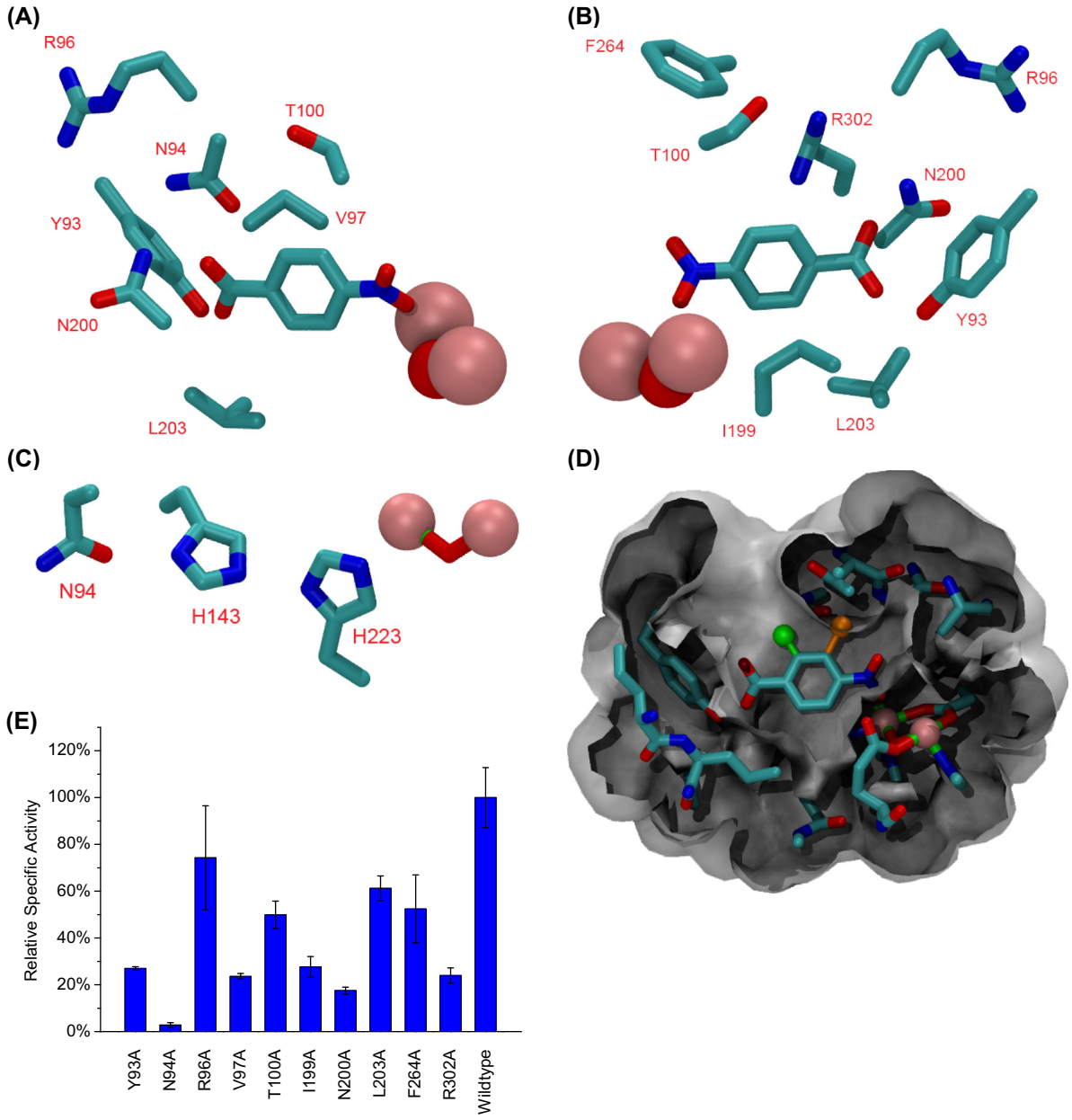

Figure 3. (A) and (B) structure of several important active-site residues in the AurF crystal structure (PDB ID: 3CHT). In all figures, active site water molecules are removed for clarity. (C) Reorientation of the N94 sidechain creates a conserved three-residue motif coupled to the active site metal. (D) Space-filling model of the AurF active site. The model clearly shows 2′ substituents (green peg) are not sterically occluded compared to 3′ substitutions (orange peg). Grey surface indicates a 1.4 Å distance from the closest residue. (D) Relative specific activity of various AurF mutants with 100 μM of PABA. Samples were tested at least three times.

data at 100 μM. From the data, compounds with substitutions at the 2′ position (**2**–**6**) retained higher activity compared to the 3′ position (**7**–**11**). Notably, compound **2** showed nearly identical activity to the native substrate. Steric and electrostatic effects are the probable reason for the preference for 2′ substituents; approach of 3′ substituted compounds towards the metal center is disfavored by steric clashes with the residues surrounding the active site (Fig. 3D), while the 2′ position is more open. The 2′ position shows a clear preference for electronegative substituents and several favorable hydrogen bonding interactions from Y93, R302, and N200 can provide additional stabilization. Compound **9** has been reported to be turned over by AurF,[11] however reliable rates could not be established as it spontaneously decomposed over the course of the assay, and putative hydroxylamine and nitro products were not observed in LC–MS analysis even when larger amounts of enzyme was added (data not shown). While compounds **7**, **8**, **10** and **29** show some activity and similar sterics, it is not certain why **9** cannot be turned over, possibly due to oxidation or decay of the compound being faster than the reaction catalyzed by AurF.

Modification of the aromatic ring and the oxidizable amine provided interesting results. Replacement of the benzene ring with a pyridine showed no activity due to decreased nucleophilicity of the pyridine analog of PABA (**13**), while substitution of ring hydrogens with fluorine was accepted by AurF (**12**). Hydroxylation of a secondary amine (**14**) proceeds slowly, while a benzylic amine **15** does not to react. The result from **12** is surprising in the fact that the reaction proceeds well with the ring polarity completely reversed, and it was previously reported that this could not occur due to the strong electron-withdrawing effects of the fluorines.[11]

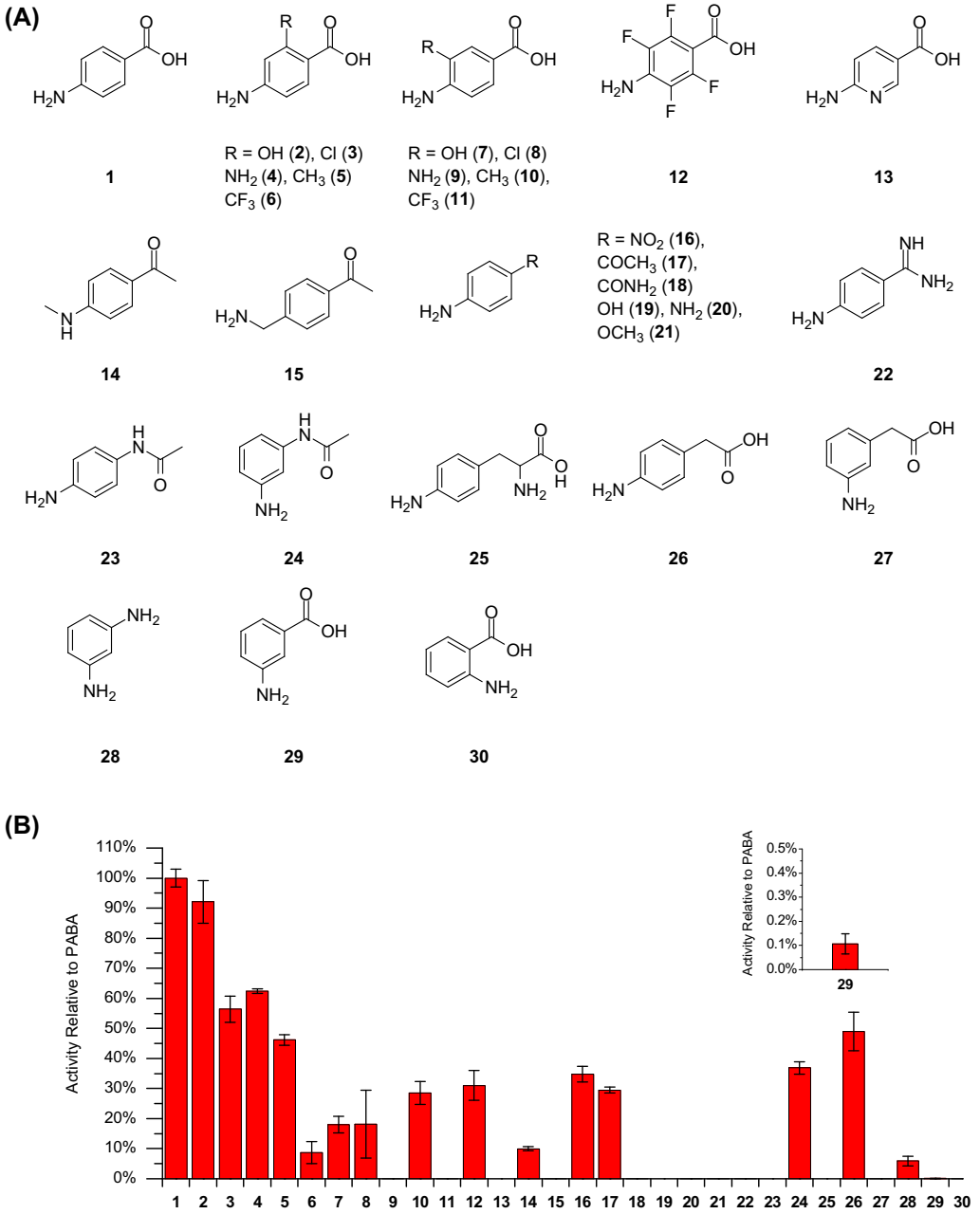

Figure 4. (A) Compounds tested with AurF in this study. (B) Relative specific activity compared to PABA (**1**). Samples were tested in triplicate with rates from no-enzyme negative controls subtracted.

As fluorine is an isostere of hydrogen, PABA and **12** are similar in size, and so the reduction in activity is not likely from steric factors. Activity towards **12** indicates that electronic state of the substrate is a major factor in the catalysis by AurF, but the enzyme itself can tolerate significantly different electronic states in its substrates. However, exaggerated electron-withdrawing effects at the 2′ (**6**) or 3′ (**11**) position gives much decreased activity. As noted in literature and as demonstrated here, the enzyme can tolerate a range of +I and −I functional groups in the substrate.

Substitution of the carboxylate end of PABA showed mixed results. In general, compounds containing a hydrogen bond acceptor (**16**–**18**, **24** and **26**) were turned over successfully by AurF, while substitutions with smaller functional groups (**19**–**21**) showed no activity. It may be assumed that compounds **19**–**21** are too far away to form effective interactions with hydrogen bonding residues such as Y93 and N200. For substrates **16**–**18**, **24** and **26**, the presence of a sp^2-hybridized oxygen is enough to act as a hydrogen bond acceptor that stabilizes the binding of the substrate enough to be turned over by the enzyme. Substrate **25** may represent an upper limit in terms of size of the compound accepted by the enzyme. In a surprising result, it was found that the regiospecificity of AurF is not strictly *para* as previously assumed.[11] Although the *ortho* isomer of PABA **30** is not turned over as a substrate, compounds **24**, **28** and **29** showed some activity, with hydroxylamine and nitro products for **14** being confirmed by LC–MS (Fig. S2). The rate of depletion of MABA (**29**) was only 0.1 % of the native substrate PABA, and could only be detected using large amounts of enzyme (20 μM). The nitrogen *meta* to the free amine in **24** and **28** seems to be important to the binding of the substrates to the active site of AurF, since the related compound

27 showed no activity. These observations indicate that amines at the 3′ position can be turned over when a nitrogen atom is present *meta* to it, but activity is severely decreased or abolished otherwise. A comparable example is seen for compounds **23** and **26**; both are structurally and sterically similar, however only the conversion of the latter is observed, since the nitrogen atoms of **23** are *para* to each other. We suggest that upon substrate binding to the active site, the nitrogen at the 1′ position hydrogen bonds in a similar manner to PABA's carboxylate. However, structural modelling of **24** and **28** gives no strong indication of the binding partners of these compounds, and the 1′ nitrogen seems not to have any significant contacts with the enzyme in the minimized structures. Some remodelling of the active site or bridging interactions with associated water molecules may explain the effect of this *meta* nitrogen.

In a few cases, there have been discrepancies between our work and literature regarding in the activity of AurF towards certain compounds. Compounds **16** and **17** have been shown by our work to be turned over by in vitro AurF (Fig. S5), while oxidation of compounds **19**, **22** and **25** could not be detected, but have previously been reported.[11,19] As **16** and **17** share similar structural features (*para*-oriented hydrogen bond acceptor) and comparable size with the native substrate, it would be unusual that they would not be transformed into nitro products by AurF, and we are able to detect at least the hydroxylamine intermediate on LC–MS. Although compound **22** is structurally and sterically quite similar to the tested compounds, the amidine group in this compound is positively charged, which may cause disfavorable electrostatic interactions with similarly charged residues R96 and R302. Therefore, it is surprising that LC–MS results from other groups have shown that it can be turned over by the wild type AurF. However, the nitro compound of **22** was only detected after reaction for 24 h with H_2O_2, prolonged conditions which we could not achieve using the PMS/NADH reaction system.[6] From literature, compound **25** has been reported to be slowly converted to its nitro product in whole-cell studies, but we could not definitively detect turnover on HPLC.[34] The activity of AurF in vivo for some *m*-substituted substrates was also determined (Fig. S6). The partial conversion of MABA (**29**) to MNBA could be observed on HPLC in an overnight incubation, collaborating results from the in vitro assay. 1,3 diaminobenzene (**28**) depletion was observed under similar conditions, but we could not definitively confirm the production of either mono or dinitro compounds. However, AurF-containing cells turned the media from clear to brown overnight, while the media did not change color in control cells, indicating an oxidation reaction specifically catalyzed by AurF involving **28**. In vivo reactions seemed to be more sensitive than in vitro assays due to longer reaction conditions and large total amounts of AurF, but overall activity may be complicated by the permeability of the substrates through the cell membrane.

3.6. Kinetic parameters of alternate substrates and mutants

Several substrates and mutants were considered for further analysis and characterization to further understand the substrate specificity and mechanism of AurF. Aside from the native substrate, three other compounds were chosen for kinetic analysis; 4-amino 2-chloro benzoic acid (**3**), 4-amino tetrafluorobenzoic acid (**12**), and 4-amino acetophenone (**17**). In all cases, the largest contributor to the lower activity compared to the native substrate is the much increased K_m, since only a 40–60% decrease in k_{cat} is observed (Table 2). Unusually, this drop in k_{cat} is similar in magnitude for all substrates and mutants tested, suggesting some sort of baseline conversion rate for the substrates tested, which is enhanced when the native substrate and enzyme are used. For compound **3**, the bulk of the chloro substituent can be accommodated by the entry pocket in the active site, and favorable interactions with the carboxylate recognizing residues are maintained (Fig. 3D). This causes relatively small changes in the K_m and k_{cat} values compared to the native substrate, which is supported by the high activity seen towards 2′ substituted compounds (Fig. 4B). Compounds **12** and **17** are isosteres of **1** and show very similar kinetic parameters to each other, however the basis for their kinetic parameters stem from different sources. The substitution of the hydroxyl group in **1** to a methyl group in **17** increases the K_m by 10-fold, indicating that hydrogen bonding plays a major role in the stabilization and binding of the substrate to the active site pocket. Electrostatics of the active site also plays a large role in substrate binding, as evidenced by compound **12**. In spite of the near-identical sterics of **1** and **12**, the K_m values for **12** are perturbed significantly, due to the reversal of polarity of the aromatic ring by fluorine substituents. However, the k_{cat} values for **12** and **17** are almost identical, indicating that electrostatic effects do not strongly affect the rate of catalysis.

A few AurF mutants were also selected for kinetic characterization. The high K_m for Y93A indicates a decreased affinity towards PABA, consistent with the role of this residue in providing hydrogen bonds to the carboxyl group. Although not directly comparable, this result is somewhat consistent with data from compound **17**; the removal of a hydrogen-bonding hydroxyl group in both cases causes large changes for K_m and k_{cat}. In the case of V97A and T100A, the major change in activity stems from a change in k_{cat}. As these residues lie near the aromatic ring of PABA in the active site, these residues were expected to show a significant change in K_m upon mutation to alanine due to the larger active site; however this change was not seen. It is unlikely that these particular residues participate in the actual mechanism of AurF, as V97 and T100 are far away from the closest metal. It has been suggested that conformational changes in the diiron cluster and possibly the active site may occur during the cycling of $Fe_2^{II/II}$ to (peroxo) $Fe_2^{III/III}$, and if so, mutations of these residues may perturb the kinetics of AurF as these conformational changes occur.[9]

4. Conclusion

In this work we have shown that AurF has an unusually low optimum pH of 5.5 and we have characterized the kinetic parameters of this enzyme at this pH. The product distribution of AurF was found to be different depending on the method of delivering reducing equivalents to the enzyme. The importance of AurF active-site residues was clarified based on site-directed

Table 2
Kinetic parameters of wildtype AurF with selected substrates, and kinetic parameters of selected AurF mutants with PABA

	PABA (**1**)	4-Amino 2-chlorobenzoic acid (**3**)	4-Amino 2,3,5,6-tetrafluorobenzoic acid (**12**)	4-Amino acetophenone (**17**)	Mutant Y93A	Mutant V97A	Mutant T100A
K_m (μM)	14.7 ± 1.1	27.1 ± 6.8	137.1 ± 14.0	214.8 ± 26.5	149.2 ± 26.0	14.9 ± 7.4	24.6 ± 4.3
k_{cat} (min^{-1})	97.4 ± 11.1	38.5 ± 0.8	42.2 ± 2.3	46.1 ± 1.2	55.4 ± 5.3	25.4 ± 1.4	47.1 ± 6.4
k_{cat}/K_m (μM^{-1} min^{-1})	6.6 ± 0.8	1.41 ± 0.35	0.147 ± 0.034	0.215 ± 0.027	0.371 ± 0.074	0.836 ± 0.420	1.93 ± 0.43

mutagenesis and substrate specificity studies. The substrate specificity of the enzyme could be rationalized from key features of the compounds tested. The regiospecificity of AurF was found not to be strictly *para*, however *meta*-substituted substrates showed much less activity. Along with kinetic studies, we have determined that the main determinant for AurF activity is the binding and affinity of the substrate in the active site. These findings will be of use in future optimization of AurF for biotechnology applications as well as further understanding of other related *N*-oxygenases.

Acknowledgements

This work was supported by a grant from the United States Office of Naval Research (N00014-02-1-0725) and Department of Chemical and Biomolecular Engineering at the University of Illinois at Urbana–Champaign (H.Z.). We thank the assistance of Dr. Lucas Li and Dr. Alex Ulanov of the Roy. J Carver Metabolomics Center for advice and technical assistance. E.C. acknowledges the support of the NIH Molecular Biophysics Training Grant.

Supplementary data

Supplementary data associated with this article can be found, in the online version, at http://dx.doi.org/10.1016/j.bmc.2014.06.002.

References and notes

1. Ju, K.-S.; Parales, R. E. *Microbiol. Mol. Biol. Rev.* **2010**, *74*, 250.
2. Winkler, R.; Hertweck, C. *ChemBioChem* **2007**, *8*, 973.
3. Lu, H.; Chanco, E.; Zhao, H. *Tetrahedron* **2012**, *68*, 7651.
4. Ferrer-Sueta, G.; Radi, R. *ACS Chem. Biol.* **2009**, *4*, 161.
5. Choi, Y. S.; Zhang, H.; Brunzelle, J. S.; Nair, S. K.; Zhao, H. *Proc. Natl. Acad. Sci. U.S.A.* **2008**, *105*, 6858.
6. Fries, A.; Winkler, R.; Hertweck, C. *Chem. Commun.* **2010**, 7760.
7. Korboukh, V. K.; Li, N.; Barr, E. W.; Bollinger, J. M.; Krebs, C. *J. Am. Chem. Soc.* **2009**, *131*, 13608.
8. Krebs, C.; Matthews, M. L.; Jiang, W.; Bollinger, J. M. *Biochemistry (Mosc.)* **2007**, *46*, 10413.
9. Li, N.; Korboukh, V. K.; Krebs, C.; Bollinger, J. M. *Proc. Natl. Acad. Sci. U.S.A.* **2010**, *107*, 15722.
10. Simurdiak, M.; Lee, J.; Zhao, H. *Chembiochem. Eur. J. Chem. Biol.* **2006**, *7*, 1169.
11. Winkler, R.; Richter, M. E. A.; Knüpfer, U.; Merten, D.; Hertweck, C. *Angew. Chem., Int. Ed.* **2006**, *45*, 8016.
12. Zocher, G.; Winkler, R.; Hertweck, C.; Schulz, G. E. *J. Mol. Biol.* **2007**, *373*, 65.
13. Jayapal, P.; Rajaraman, G. *Phys. Chem. Chem. Phys.* **2012**, *14*, 9050.
14. McIlvaine, T. C. *J. Biol. Chem.* **1921**, *49*, 183.
15. Copeland, R. A. *Enzymes: A Practical Introduction to Structure, Mechanism, and Data Analysis*; John Wiley and Sons, 2000.
16. Humphrey, W.; Dalke, A.; Schulten, K. *J. Mol. Graphics* **1996**, *14*, 27.
17. Comeau, S. R.; Gatchell, D. W.; Vajda, S.; Camacho, C. J. *Nucleic Acids Res.* **2004**, *32*, W96.
18. Kawai, S.; Kobayashi, K.; Oshima, T.; Egami, F. *Arch. Biochem. Biophys.* **1965**, *112*, 537.
19. Platter, E.; Lawson, M.; Marsh, C.; Sazinsky, M. H. *Arch. Biochem. Biophys.* **2011**, *508*, 39.
20. Kontro, M.; Lignell, U.; Hirvonen, M.-R.; Nevalainen, A. *Lett. Appl. Microbiol.* **2005**, *41*, 32.
21. Corvini, P. F. X.; Gautier, H.; Rondags, E.; Vivier, H.; Goergen, J. L.; Germain, P. *Microbiology* **2000**, *146*, 2671.
22. Willing, A.; Folmann, H.; Auling, G. *Eur. J. Biochem.* **1988**, *175*, 167.
23. Luykx, D. M. A.; Prenafeta-Boldú, F. X.; de Bont, J. A. *Biochem. Biophys. Res. Commun.* **2003**, *312*, 373.
24. Patel, R. N.; Hou, C. T.; Laskin, A. I.; Felix, A. *Appl. Environ. Microbiol.* **1982**, *44*, 1130.
25. Winkler, R.; Zocher, G.; Richter, I.; Friedrich, T.; Schulz, G. E.; Hertweck, C. *Angew. Chem., Int. Ed.* **2007**, *46*, 8605.
26. Bailey, L. J.; Fox, B. G. *Biochemistry (Mosc.)* **2009**, *48*, 8932.
27. Kumar, R. P.; Ravindranath, S. D.; Vaidyanathan, C. S.; Rao, N. A. *Biochem. Biophys. Res. Commun.* **1972**, *48*, 1049.
28. Halliwell, B. *Biochem. J.* **1977**, *167*, 317.
29. Fries, A.; Bretschneider, T.; Winkler, R.; Hertweck, C. *ChemBioChem* **2011**, *12*, 1832.
30. Das, D.; Eser, B. E.; Han, J.; Sciore, A.; Marsh, E. N. G. *Angew. Chem., Int. Ed.* **2011**, *50*, 7148.
31. Tinberg, C. E.; Lippard, S. J. *Acc. Chem. Res.* **2011**, *44*, 280.
32. Jakopitsch, C.; Auer, M.; Regelsberger, G.; Jantschko, W.; Furtmüller, P. G.; Rüker, F.; Obinger, C. *Eur. J. Biochem.* **2003**, *270*, 1006.
33. Schuller, D.; Ban, N.; Vanhuystee, R.; Mcpherson, A.; Poulos, T. *Structure* **1996**, *4*, 311.
34. Kawai, S.; Oshima, T.; Egami, F. *Biochim. Biophys. Acta* **1965**, *97*, 391.